European Journal of Human Genetics (2010) 18, 985–992

www.nature.com/ejhg

ARTICLE

Pelizaeus–Merzbacher-like disease is caused not only by a loss of connexin47 function but also by a hemichannel dysfunction

Simone Diekmann[1], Marco Henneke[1], Birgitta C Burckhardt[2] and Jutta Gärtner*[,1]

Autosomal recessive mutations in the *GJA12/GJC2* gene encoding the gap junction protein connexin47 (C×47) cause a form of Pelizaeus–Merzbacher-like disease (PMLD) with hypomyelination, nystagmus, impaired psychomotor development and progressive spasticity. We investigated the functional consequences of four C×47 missense mutations (G149S, G236R, T265A, and T398I) and one C×47 complex mutation (A98G_V99insT) by immunoblot analysis and immunocytochemistry in transfected communication-incompetent HeLa cells and in OLI-neu cells. All studied C×47 mutants, except G236R, generated stable proteins in transfected HeLa cells and OLI-neu cells. The mutants T265A and A98G_V99insT were retained in the ER, T398I formed gap junctional plaques at the plasma membrane, and G149S showed both, structures at the plasma membrane and ER localization. Two-microelectrode voltage clamp analyses in *Xenopus laevis* oocytes injected with wild-type and mutant C×47 cRNA revealed reduced hemichannel currents for G236R, T265A, and A98G_V99insT. In contrast, T398I revealed hemichannel currents comparable to wild-type. For C×47 mutant T398I, our results indicate a defect in hemichannel function, whereas C×47 mutants G149S, G236R, T265A, and A98G_V99insT are predicted to result in a loss of C×47 hemichannel function. Thus, PMLD is likely to be caused by two different disease mechanisms: a loss of function and a dysfunction.
European Journal of Human Genetics (2010) **18,** 985–992; doi:10.1038/ejhg.2010.61; published online 5 May 2010

Keywords: leukodystrophy; Pelizaeus–Merzbacher-like disease; GJA12/GJC2 mutations; connexin47; voltage clamp analysis

INTRODUCTION

Pelizaeus–Merzbacher Disease (PMD; MIM no. 312080), the prototype of hypomyelinating disorders, is due to X-linked recessive rearrangements or mutations of the *proteolipid protein* (*PLP1*) gene.[1] Clinical features of the classical form comprise nystagmus and impaired psychomotor development within the first months of life followed by progressive spasticity and cerebellar signs. Pelizaeus–Merzbacher-like disease (PMLD, MIM no. 608804) shows clinical and neuroradiologic features, such as classic PMD, but is not associated with *PLP1* molecular defects.[2] Recessive mutations in the *GJA12* gene, recently renamed *GJC2* (http://www.genenames.org/genefamily/gj.php), cause one form of PMLD.[3] This gene encodes gap junction protein connexin47 (C×47). Until now 23 different *GJA12/GJC2* mutations have been reported.[3–9]

Gap junctions (GJs) are specialized channels between apposed cells allowing direct metabolic and electrical communication between most cell types in mammalian tissues by passive diffusion of molecules smaller than 1000Da. This gap junction intercellular communication (GJIC) has an important role in essential cellular processes, such as development, proliferation, differentiation, and cell death.[10] Gap junctions are highly specialized structures, consisting of two hemichannels of apposing cells. Several thousand GJ channels assemble to gap junctional plaques. The hemichannel (connexon) in the plasma membrane is formed by six connexins. Connexins, highly conserved integral membrane proteins, have four transmembrane domains, two extracellular loops and three cytoplasmic components, one amino- and carboxy-terminal region, and a cytoplasmic loop. Homotypic GJs consist of hemichannels with one type of connexins, whereas heterotypic GJs are formed by hemichannels with different connexins.[11] So far, 20 *connexin* genes have been described in mouse and 21 in human genome. More than half of them are expressed in the nervous system.[12]

Astrocytes and oligodendrocytes are coupled by GJs forming part of the 'panglial syncytium'.[13] Gap junction intercellular communication occurs between oligodendrocytes and astrocytes (O/A) and adjacent astrocytes (A/A), but there is no evidence for GJs between adjacent oligodendrocytes in mice.[13–16] Oligodendrocytes express C×47, C×32, and C×29,[16,17] whereas astrocytes express C×26, C×30, and C×43.[18,19] The O/A coupling is mediated by heterotypic channels between C×47/C×43 and C×32/C×30, both appearing to be essential for the proper maintenance of myelin.[20] So far, C×47 mutants have been shown to result in loss of function, suggesting an impaired O/A coupling mediated by C×47/C×43.[21] Here, we provide further evidence that loss of C×47 function causes PMLD. However, our results further suggest a second disease mechanism, namely a C×47 hemichannel dysfunction.

MATERIALS AND METHODS

Wild-type and mutant expression constructs

The full length C×47 (1–1320 bp, 1–439 aa, RefSeqID *NM_020435.2*) was PCR amplified from wild-type cDNA and cloned into the mammalian expression

[1]Department of Pediatrics and Pediatric Neurology, Georg August University, Göttingen, Germany; [2]Department of Physiology and Pathophysiology, Georg August University, Göttingen, Germany
*Correspondence: Professor J Gärtner, Department of Pediatrics and Pediatric Neurology, Georg August University, Robert-Koch-Strasse 40, 37075 Göttingen, Germany. Tel: +49 551 398035; Fax: +49 551 396252; E-mail: gaertnj@med.uni-goettingen.de
Received 29 June 2009; revised 1 April 2010; accepted 1 April 2010; published online 5 May 2010

vector pcDNA3.1+ (Invitrogen, Karlsruhe, Germany). Site-directed mutagenesis was performed using the FlipFlop Site-Directed Mutagenesis Kit (Bioline, Luckenwalde, Germany). Wild-type C×47 with the alternative start codon (10–1320 bp, 4–439 aa) was also cloned into pcDNA3.1+.

Generation of C×47 antiserum

Polyclonal rabbit antiserum against human C×47 was generated by conventional methods using glutathione-*S*-transferase (GST) fusion protein as immunogen (Seramun, Heidesee, Germany). A fragment of the intracellular loop (310–591 bp, 104–197 aa) was amplified using wild-type C×47 construct as template. The PCR product was subcloned into the pGEX-KG vector that encodes for GST. The GST fusion protein was expressed by BL21 bacteria (Bioline) and purified using glutathione–Sepharose4B (GEHealthcare, München, Germany). Final bleed serum was used for immunoblot analysis at dilution 1:10 000. This antiserum did not work properly in immunoblot analysis of oocyte lysates.

Immunoblot analysis

HeLa cells were cultured in Dulbecco's modified Eagle's medium containing 10% fetal bovine serum at 37 °C and 5% CO_2. Transfection was carried out using the Effectene Kit (Qiagen, Hilden, Germany). Transfected HeLa cells were collected at 48 h after transfection and lysed in RIPA buffer (150 mM NaCl; 50 mM Tris–HCl; 5 mM EDTA; 0.5% Na-deoxycholate; 1% NP-40; 0.1% SDS; protease inhibitor cocktail). Immunoblot analyses were performed using standard techniques. Horseradish peroxidase-conjugated secondary antibodies were used to view bound primary antibodies (C×47 antiserum) using Lumi-Light Western Blotting Substrate (Roche, Mannheim, Germany). Chemiluminescence signals were analysed using the Luminescent Image Analyzer, LAS-4000mini (Fujifilm, Düsseldorf, Germany).

Immunocytochemistry

An immortalized oligodendrocyte precursor cell line, OLI-neu,[22] was cultured in Sato medium containing 1% horse serum on poly-(L-lysine)-coated culture dishes at 37°C and 5% CO_2. The OLI-neu cells were transfected with FuGENE-HD (Roche, Germany). HeLa and OLI-neu cells transfected with wild-type or mutant C×47 were fixed at 20–48 h after transfection with 4% paraformaldehyde/PBS. Immunostaining was done using standard methods with the C×47 antiserum (dilution 1:2000) and with anti-Pan-Cadherin (plasma membrane marker, Abcam, Cambridge, UK) and anti-PDI (ER marker, Abcam) antibodies to detect co-localization. Alexa488- and Cy3-conjugated anti-rabbit and anti-mouse secondary antibodies were used (Molecular Probes, Karlsruhe, Germany and Jackson ImmunoResearch, Suffolk, UK; diluted 1:1000 and 1:500, respectively). The cells were embedded in ProLongGold mounting medium with DAPI (Invitrogen). Fluorescence signals were detected using fluorescence microscope Axio-Imager M.1 (Zeiss, Göttingen, Germany).

Oocyte preparation and microinjection

The stage V and VI oocytes from *Xenopus laevis* (Nasco, Fort Atkinson, WI, USA) were separated by treatment with collagenase (TypCLS II, Biochrom, Berlin, Germany) and maintained at 16–18°C in a daily-replaced control solution (in mM): 110 NaCl, 3 KCl, 2 $CaCl_2$, 5 HEPES (pH 7.5), supplemented with sodium pyruvate (0.55 mg/ml) and gentamycin (50 μg/ml). An antisense oligonucleotide complementary to *Xenopus* C×38 mRNA (asC×38) was synthesized: 5′-gctttagtaattcccatcctgccatgtttcc-3′ (Metabion, Martinsried, Germany).[23] To deplete endogenous C×38 expression, asC×38 was injected (23 nl, 1 ng/nl) into oocytes 1 day after the removal from the frog and 48–72 h before recording. To analyze the function of C×47 wild-type and mutant hemichannels in oocytes, cRNA transcription was performed *in vitro*, using the SP6 mMessage mMachine Kit (Ambion, Foster City, CA, USA). The cRNA (5 ng per oocyte) was co-injected with asC×38.

Electrophysiological studies

Resting membrane potentials and non-junctional transmembrane currents in single oocytes were studied by two-electrode voltage clamp (TEVC) technique using a commercial amplifier (OC-725C, Warner, Hambden, CT, USA). The microelectrodes were filled with 3 M KCl and had resistances of less than 1 MΩ. Oocytes were superfused with external bath solution (control solution without

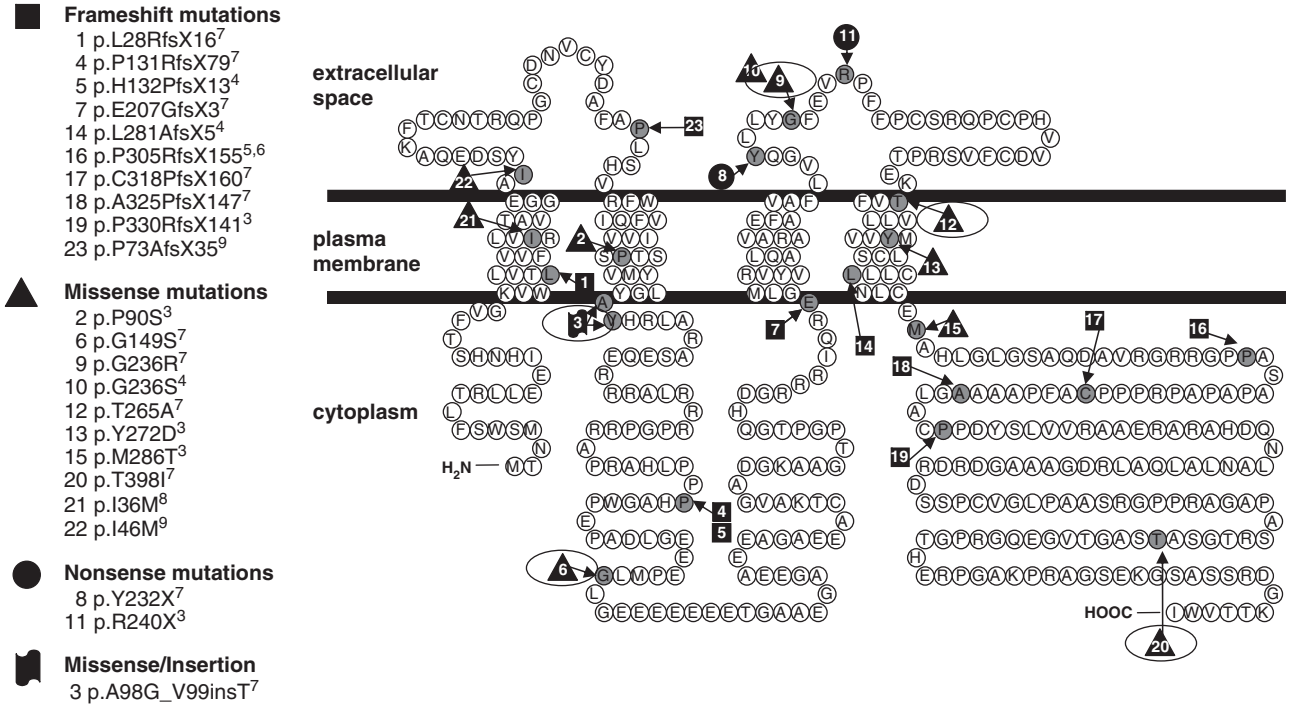

Figure 1 Membrane topology and localization of all known *GJA12/GJC2* mutations. Seven mutations are observed on the four membrane-spanning domains, six on the intracellular loop, four on the extracellular loop, and six on the cytoplasmic carboxy-terminus. The five mutations characterized in this study are encircled. Mutations are designated according to current guidelines of international mutation nomenclature. Designation of the mutation p.P305RfsX155[6] and of the mutation p. P73AfsX35[9] was changed according to current guidelines of mutation nomenclature.

sodium pyruvate and gentamycin). After stabilization of the membrane potential, single oocytes were clamped to −40 mV. Superfusion was switched after 200 s to calcium-free bath solution. Non-junctional transmembrane currents were measured after 5 min. A depolarization pulse to 0 mV was applied to the oocyte and transmembrane currents were measured after 100 s. All currents were measured at a saturation of about 100% (see Supplementary Figure 1). At −40 mV, calcium-activated chloride currents are mostly inactivated.[24] Channel opening is blocked by external divalent cations (ie, Ca^{2+}) and in most cases by hyperpolarizing transmembrane potentials.[25]

The data were corrected by subtracting the average leakage current measured in control oocytes (only injected with asC×38). Some outliers were excluded using the Nalimov outlier test. An unpaired Student's *t*-test was probed.

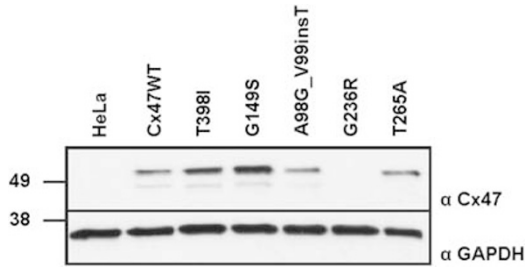

Figure 2 Immunoblot analysis of C×47 expression in transfected communication incompetent HeLa cells. Immunoblot analysis was probed with HeLa cells transiently transfected with wild-type C×47 (C×47WT), mutant C×47 (T398I, G149S, A98G_V99insT, G236R, and T265A) and with untransfected HeLa cells (HeLa). Immunoblots were probed with a rabbit antiserum against human C×47 (1:10 000) and a monoclonal GAPDH antibody (Abcam, 1:5000).

RESULTS

Expression of wild-type and mutant C×47 in HeLa cells

We analyzed the functional consequences of four missense mutations G149S, G236R, T265A, and T398I and one complex mutation A98G_V99insT with an amino-acid substitution followed by an amino-acid insertion, as previously described.[7] The localization within the different protein domains is illustrated in Figure 1 and is one criterion to study these five distinct missense mutations. To determine whether selected mutations affect protein expression, immunoblot analysis of transfected HeLa cells was performed (Figure 2). The wild-type and all mutants except G236R were detected by the C×47 antiserum. There was no signal in untransfected HeLa cells, indicating the specificity of the C×47 antiserum.

Intracellular localization of wild-type and mutant C×47 in HeLa and OLI-neu cells

A second alternative C×47 start codon, nine nucleotides downstream from the first ATG, was described.[21] We analyzed the expression and localization of the constructs with the first and the second start codon by immunostaining transfected HeLa and OLI-neu cells. C×47 proteins were immunolabeled with the C×47 antiserum and visualized using epifluorescence microscopy (Figure 3). There was no difference in subcellular localization: both proteins were found in punctate structures localized to the plasma membrane. Therefore, all constructs analyzed in this study were cloned starting from the first ATG. Accordingly, our description of nucleotide and amino-acid positions, including the designation of mutations refers to the first upstream ATG.

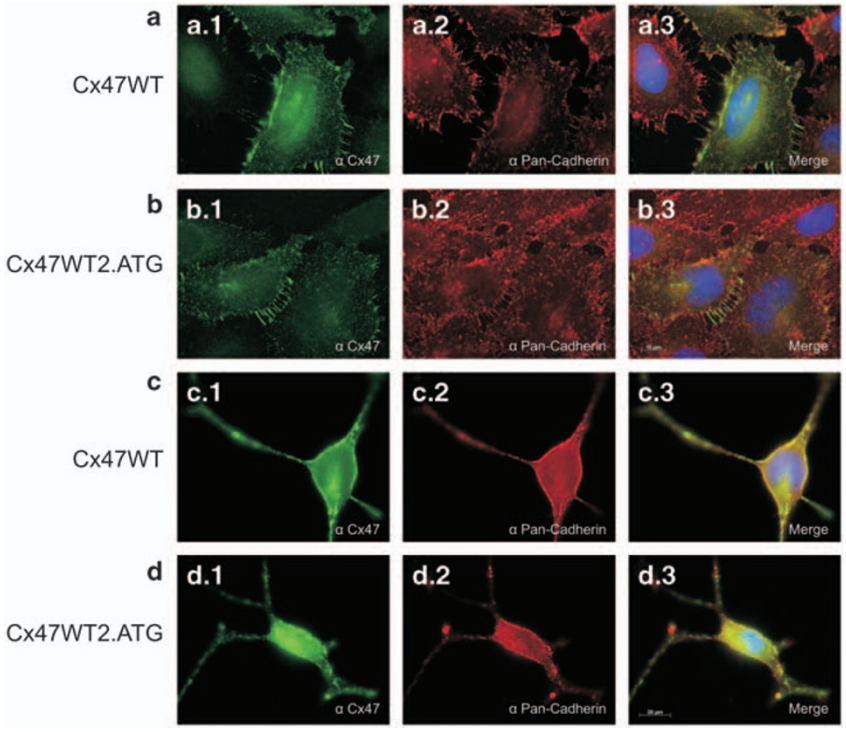

Figure 3 Subcellular localization of wild-type C×47. Double-staining immunofluorescence microscopy studies in communication incompetent HeLa cells (**a** and **b**) and OLI-neu cells (**c** and **d**) transiently transfected with wild-type C×47 first ATG (C×47WT; **a** and **c**) and alternative second ATG (C×47WT2.ATG; **b** and **d**). Transfected cells were immunolabeled with a rabbit antiserum against human C×47 (green) and a mouse monoclonal antibody against the plasma membrane protein Pan-Cadherin (red). Gap junctional plaques were seen at the plasma membrane for cells expressing wild-type C×47 from the first ATG and for cells expressing wild-type C×47 from the alternative second ATG.

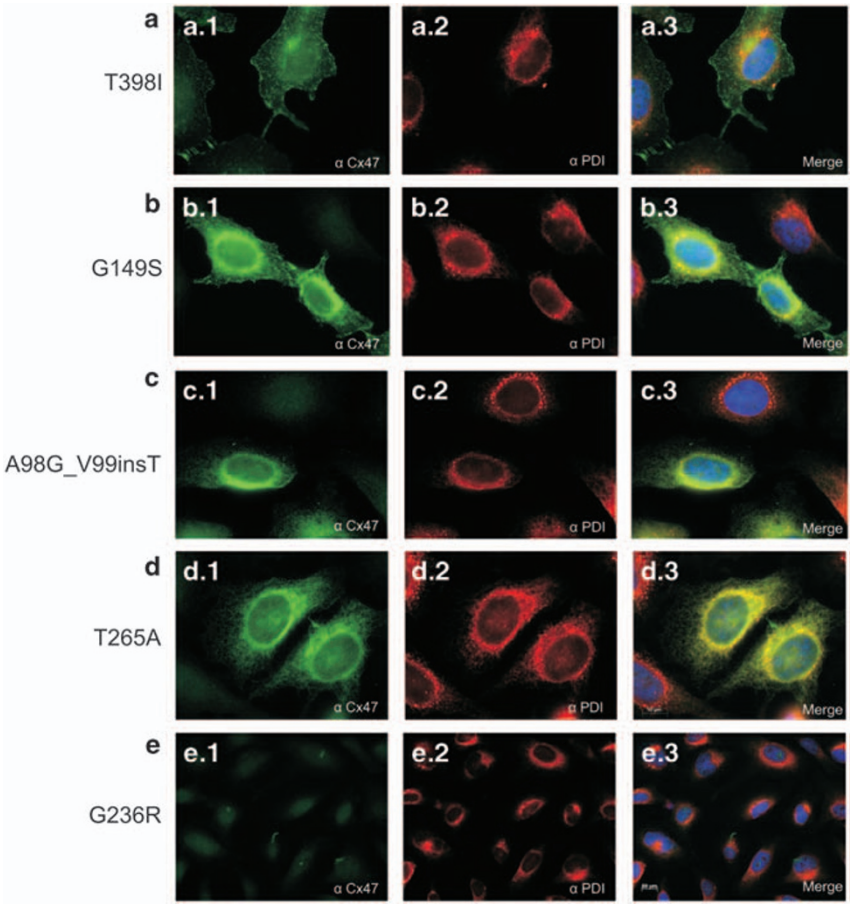

Figure 4 Subcellular localization of mutant C×47 in HeLa cells. Communication incompetent HeLa cells transiently transfected with mutant C×47 (T398I, G149S, A98G_V99insT, T265A, and G236R) were immunolabeled with a rabbit antiserum against human C×47 (green) and a mouse monoclonal antibody against the ER protein disulfide isomerase (α PDI, red). Gap junctional plaques were seen at the plasma membrane for cells expressing mutant T398I and G149S (**a** and **b**). There was also partial co-localization with the ER marker for both mutants, but the ER co-localization was even higher for the mutant G149S. Nearly perfect ER co-localization was seen for the mutants A98G_V99insT and T265A (**c** and **d**). As expected, there was no signal for mutant G236R (**e**).

To examine whether the C×47 mutants were properly targeted to the plasma membrane, HeLa and OLI-neu cells, transfected with one of the mutant constructs, were immunolabeled with the C×47 antiserum (Figures 4 and 5). Double-staining immunofluorescence studies revealed differences in the subcellular localization of C×47 mutants compared with wild-type protein. As expected, wild-type C×47 was found in punctate structures co-localizing to the plasma membrane. These structures are assumed to represent gap junctional plaques. The mutant, T398I, was labeled as punctate structures predominantly at the plasma membrane (Figures 4a and 5a). However, there was also a faint co-localization to the ER. HeLa and OLI-neu cells expressing G149S showed punctate structures at the plasma membrane and in the ER (Figures 4b and 5b). The mutants A98G_V99insT and T265A were only localized to the ER (Figures 4c, d, 5c and d). As expected, there was no fluorescence signal in G236R-transfected (Figures 4e and 5e) and in untransfected HeLa and OLI-neu cells (data not shown).

Functional characterization of wild-type and mutant C×47 in *Xenopus laevis* oocytes

Resting membrane potentials and non-junctional transmembrane currents in single oocytes were studied by two-electrode voltage clamp (TEVC) technique. Average resting membrane potentials upon superfusion with calcium-containing solution for oocytes injected with asC×38 and wild-type C×47 cRNA (WT) or mutant C×47 cRNA (G149S, A98G_V99insT, G236R, and T265A) ranged from -35.4 ± 0.8 to -39.2 ± 0.9 mV (Figure 6a). There was no significant change of resting membrane potential compared with wild type; only for those 84 oocytes injected with T398I, a significant decreased potential was observed (-30.4 ± 0.9 mV, $P=0.0001$). Resting membrane potential from 79 control oocytes showed a small significant hyperpolarization (-41.9 ± 0.9 mV, compared with wild-type -39.2 ± 0.9 mV, $P=0.025$). The injected oocytes were clamped to -40 mV and superfused with calcium-free solution. They showed slowly activated inward currents that were reversibly inactivated when calcium-free solution was replaced. The amplitude of wild-type calcium-sensitive hemichannel currents after subtracting the average leakage current measured in control oocytes was -554 ± 49 nA (ΔI_m, Figure 6b). In T398I-injected oocytes, ΔI_m represented -693 ± 58 nA. There is no significant difference between corrected wild-type and T398I hemichannel currents ($P=0.0826$). Significantly reduced transmembrane currents were observed for G149S, A98G_V99insT, G236R, and T265A ($P \leq 0.0012$, compared with wild-type). Application of depolarization step to 0 mV elicited an

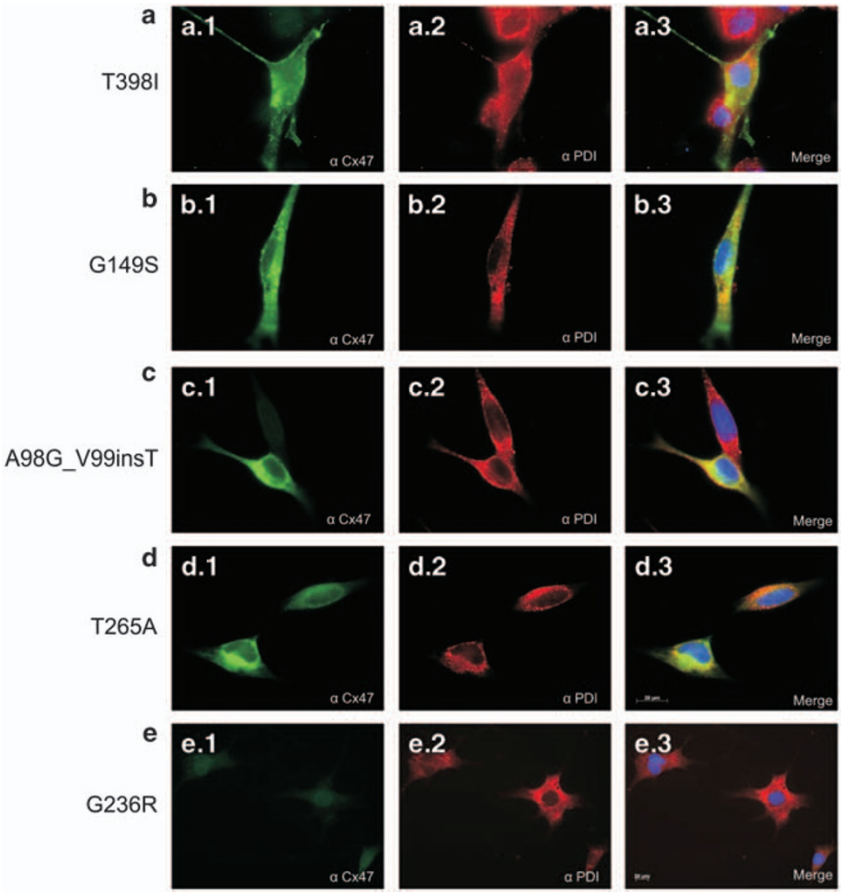

Figure 5 Subcellular localization of mutant C×47 in OLI-neu cells. OLI-neu cells transiently transfected with mutant C×47 (T398I, G149S, A98G_V99insT, T265A, and G236R) were immunolabeled with a rabbit antiserum against human C×47 (green) and a mouse monoclonal antibody against the ER protein disulfide isomerase (α PDI, red). Similar to in HeLa cells gap junctional plaques were observed at the plasma membrane for OLI-neu cells expressing mutant T398I and G149S (**a** and **b**). There was also partial co-localization with the ER marker for both mutants, but the ER co-localization was even higher in the mutant G149S. Nearly perfect ER co-localization was seen for the mutants A98G_V99insT and T265A (**c** and **d**). As expected, no signal for mutant G236R could be detected (**e**).

instantaneous increment of outward calcium-sensitive currents in oocytes, injected with wild-type C×47 cRNA (ΔI_m=406 ± 36 nA, Figure 6c). No depolarizing activation was observed for T398I hemichannel currents average (ΔI_m=162 ± 18 nA). Transmembrane currents observed for G149S, A98G_V99insT, G236R, and T265A were significantly reduced (below 75 nA; P=0.0001). The transmembrane currents varied considerably in magnitude, indicating that conductance of oocytes changed according to the cRNA injected.

DISCUSSION

A second alternative start codon for C×47, nine nucleotides downstream from the first ATG, was described.[21] So far, there is no experimental evidence regarding which ATG of C×47 is the translation initiation codon. Therefore, we analyzed the expression and subcellular localization of both using constructs with the first and the second start codon. Interestingly, we saw no difference in subcellular localization. Both proteins localized to the plasma membrane in HeLa cells. Whether one or both start codons are translated and whether the downstream ATG is more favourable is still unknown.[26] Furthermore, it needs to be investigated whether a tissue-specific translation exists. Reference sequence *NM_020435.2* (NCBI database) declares the upstream ATG to be the putative start codon. All constructs analyzed in this study were cloned starting from the first ATG.

Besides G149S, all studied missense mutations affect highly conserved amino acids, indicating evolutionarily constrained key residues for protein function.[7] All C×47 mutants, except G236R, were able to generate stable proteins in transfected HeLa cells. The G236R mutation leads to an amino-acid substitution of neutral glycine against alkaline arginine in the second highly conserved extracellular domain. There are six highly conserved cysteines in both extracellular domains thought to be essential for connexin stabilization, connexin formation, and connexon docking.[27] The G236R substitution is located close to C245. Presumably, this mutation inhibits the formation of an important disulfide bond and leads to instability of C×47, resulting in early degradation during translation. The degradation results in lack of this protein in the plasma membrane and may inhibit C×47/C×43 heterotypic GJIC between oligodendrocytes and astrocytes.[20] For PMD, it was shown that mutations mapping into the extracellular loop region of PLP/DM20 lead to the failure of oligodendrocytes to form correct intramolecular disulfide bonds and result in activation of the unfolded protein response (UPR).[28] Interestingly, point mutations in the second extracellular domain of C×43 are known to cause Oculodentodigital Dysplasia (ODDD) preventing C×43 localization to the plasma membrane and consecutive loss of function.[29]

The mutation, T398I, located in the C-terminus, does not alter the localization of C×47 to the plasma membrane and apparently does not inhibit hemichannel function. The C-terminus contains multiple

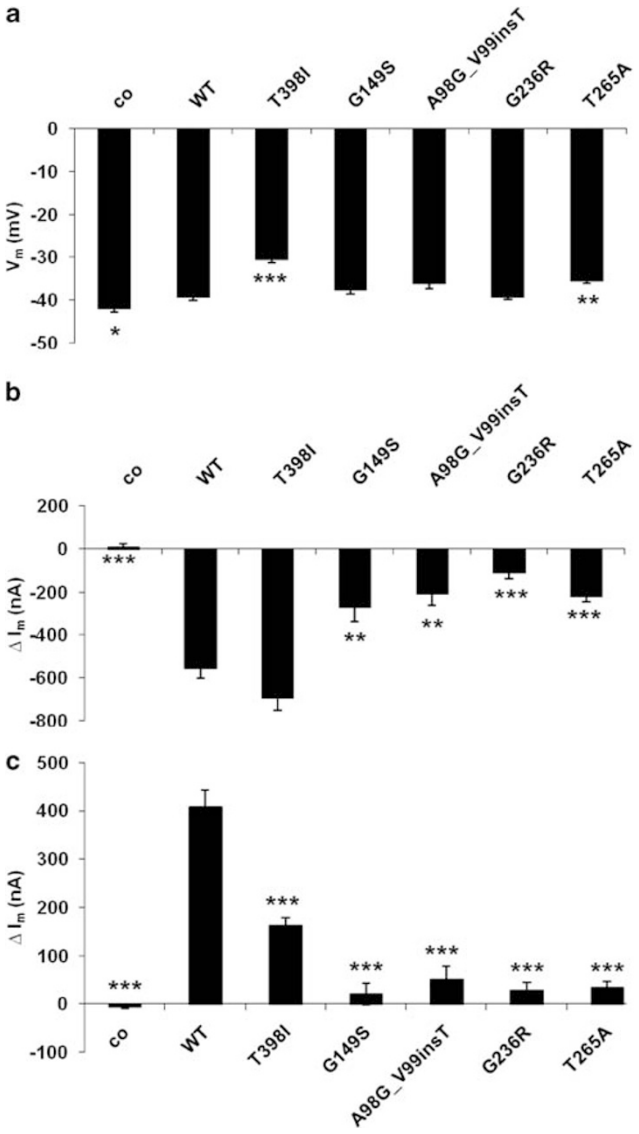

Figure 6 Electrophysiological studies of oocytes injected with wild-type and mutant C×47 cRNA. Resting membrane potentials and non-junctional transmembrane currents were measured by two-electrode voltage-clamp techniques. Resting membrane potentials (V_m) were recorded in control oocytes (co, injected with asC×38 only, n=79), wild type (WT, n=84) and mutant (T398I, n=84; G149S, n=37; A98G_V99insT, n=34; G236R, n=40; and T265A, n=53) C×47-expressing oocytes (in addition, injected with asC×38) during perfusion with calcium-containing solution (**a**). Membrane currents were monitored in control oocytes, wild-type, and mutant C×47-expressing oocytes (additionally injected with asC×38) clamped at −40 mV (**b**) or at 0 mV (**c**) during perfusion with calcium-free solution. All experimental data are averages of different numbers of oocytes (n=34–84) from at least three different donors. The data were corrected for leakage by subtracting the average leakage current measured in control oocytes (ΔI_m). Statistical analysis was done by an unpaired Student's t-test compared with wild-type. Errors are given as SEM. The P-values (*$P \leq 0.026$; **$P \leq 0.0032$; ***P=0.0001) were adjusted according to Bonferroni.

phosphorylatable serine, threonine, and tyrosine residues that are considered an intrinsic part of the voltage and low pH gate for various GJ channels.[30] The C-terminal mutations in the *C×43* gene were identified in patients with heart malformation and defects in laterality.[31] In these cases, one or more C-terminal phosphorylatable serine or threonine residues were substituted. Mutant transfectants were demonstrated to have normal levels of GJIC but abnormalities in its regulation. Furthermore, mutations in the C-terminus of *C×32* are thought to affect functional regulation of GJs.[32,33] Using TEVC, we observed the depolarization of resting membrane potential in oocytes injected with T398I. This observation leads to the hypothesis that T398I hemichannel opening occurs incidentally. Consequently, this mutant may affect oligodendrocytes causing leakage across the plasma membrane through opening hemichannels. Presence of open hemichannels was shown for other connexins and postulated as a possible mechanism of cell injury and cell death in other tissues.[34,35] Therefore, a regulation defect of C×47 hemichannel function in mutant T398I is likely.

Mutation G149S lies within the less conserved intracellular protein domain. It co-localized to the ER and partially also to the plasma membrane. Hemichannel currents were nearly absent. The weak transmembrane currents could be caused by the formation of non-functional hemichannels, by aggregation of connexins in the ER preventing the assembly of hemichannels at the plasma membrane, or by unspecific currents higher than those for control oocytes. Faint transmembrane currents were also observed for other mutants localized to the ER (T265A and A98G_V99insT) and for G236R that did not express any protein product. Thus, these currents represent rather unspecific currents.

Both mutations, T265A and A98G_V99insT, located in the transmembrane domains, showed significantly reduced hemichannel currents and were not able to form homomeric hemichannels. Both were retained in the ER. The mutations, P90S, Y272D, and M286T, also located close to or directly at the transmembrane domains, showed aggregation of mutated connexins in the ER and loss of C×47 function.[21] For the transmembrane domains three and four of C×32, an important role in protein trafficking has been proposed.[36] Therefore, mutations in the transmembrane domains of C×47 might basically inhibit protein transport.

Two alternative pathomechanisms are considered to be responsible for GJA12/GJC2-associated PMLD. Similar to several previously described alterations our mutants: G149S, G236R, T265A, and A98G_V99insT cause PMLD most likely by loss of C×47 function. In contrast, T398I does not lead to loss of function but might result in a hemichannel dysfunction, indicating a second and new disease mechanism in GJA12/GJC2-associated PMLD.

Clinical features of patients carrying the characterized mutations previously described by our group are listed in Table 1. Mutations G149S, T265A, and A98G_V99insT were found at heterozygous state in four families; thus a genotype–phenotype correlation cannot be done for these alterations as the second allele may modulate the expression of the first one. Mutations T265A and G236R were identified at homozygous state in two families. Both alterations result indeed in a loss of C×47 function, but only mutant G236R was not detected as stable protein in our experiments. The residual protein expressed for mutant T265A likely results in the milder phenotype of subject G330. However, more homozygous patients and the functional consequences of their mutations must be analyzed to definitely assess a genotype–phenotype correlation in this disorder.

Mutants P90S, Y272D, and M286T do not efficiently form functional heterotypic C×47/C×43 GJs, suggesting that disruption of these channels affects human myelination and cause GJA12/GJC2-associated PMLD.[20,37] Mice lacking C×47 were viable and fertile and showed no obvious morphological or behavioral abnormalities,[17] whereas animals lacking C×47 and C×32 developed a profound CNS demyelination.[16] Potentially, C×30/C×32 could compensate

Table 1 Clinical data of patients and functional consequences of C×47 mutations

Patient/sex	Age at disease onset, month	Age at last examination	Score of best motor function[a] (age at walking, year)	Speech (age > 1 year)	Education (age > 5 year)	Course	Age at onset of motor degradation, year	Age at onset of speech deterioration, year	Mutation at nucleotide level	Mutation at protein level	Mutant alleles	Localization of C×47	Functional defect of C×47
mt3548/M	9	7	1	+ (D)	Special school	S	—	—	c.1193C>T	p.T398I	Het	PM	Dysfunction
G218/M	12	6	4 (2)	+ (D)	Regular school	SD	5	—	c.1193C>T	p.T398I	Het	PM	Dysfunction
G344/M	3	1	2			SI	—	—	c.445G>A	p.G149S	Het	ER, PM	Loss of function
mt3550/M	9	5	2	+	Special school	S	—	—	c.292_293 insGTA	p.A98G_V99 insT	Het	ER	Loss of function
G330/F	1	17	4 (3.5)	+ (D)	Regular school	SD	8 (wcb 10)	11	c.793A>G	p.T265A	Hom	ER	Loss of function
G193/M	12	14	2	+ (D; BD)	Special school	SD	4	12	c.706G>C	p.G236R	Hom	ND	Loss of function

Mutations and clinical data previously described and published by our group.[7] Mutation nomenclature is based on GJA12/GJC2 cDNA sequence (RefSeq NM_020435.2), +1 corresponds to the A of the first ATG.
[a]Disease forms according to a development score (best motor function acquired): 0=no motor achievement; 1=head control; 2=sitting without aid; 3=walking with aid; 4=walking independently.
BD, buccofacial dyspraxia; D, dysarthria; ER, endoplasmatic reticulum; F, female; M, male; Het, heterozygous; Hom, homozygous; ND, not detectable; PM, plasma membrane; S, stable; SD, slow degradation; SI, slow improvement; wcb, wheelchair bound.

the lack of C×43/C×47 GJs in mice.[20] However, there is no evidence for such a compensatory mechanism in humans. Furthermore, C×47/C×43 and C×32/C×30 channels were described to have different roles in O/A coupling in primates.[37] Thus, PMLD is likely caused by loss of function for mutants expressing no proteins and for mutants retained in the ER. However, mutants assembling in the ER, as shown for T265A and A98G_V99insT in our study and as previously shown for P90S, Y272D, and M286T,[21] could also induce a pathological activation of UPR, resulting in changes of cell physiology (ie apoptosis, abnormal differentiation, and altered proliferation). Although no experimental evidence for this putative pathomechanism was found in a cell model system analyzing the PERK–UPR pathway, the authors Orthmann-Murphy *et al*. did not rule out that C×47 activates a different UPR-related pathway.[21] For PLP1 mutants causing PMD and for mutants of peripheral myelin protein (PMP22) causing Charcot–Marie–Tooth type 1A (CMT1A) chronic, pathological activation of UPR by accumulation of misfolded and undegraded proteins in the ER has been postulated.[38–41] The activation of UPR by certain PLP1 mutants may result in oligodendrocyte cell death affecting the myelination process.[42] Toxic accumulation of C×32 in the ER has also been suggested as a pathomechanism for some X-linked Charcot–Marie–Tooth (CMTX) C×32 mutants.[36] These authors postulated that inherited diseases of myelin share common pathophysiology in which mutant protein retained in intracellular compartments has deleterious effects on the protein folding, degradation, or trafficking machineries. Potentially, there is co-action of both, loss of ability to form O/A heterotypic GJs and toxic ER accumulation. Moreover, it is possible that oligodendrocyte and astrocyte connexins have roles besides forming GJs.[37]

The O/O coupling in humans has not been examined, so it might be possible that C×47 GJs exist between adjacent oligodendrocytes unlike shown in rodents.[37] In addition to C×47/C×43 dysfunction, abnormal homotypic C×47 GJs between oligodendrocytes and myelin sheets could be responsible for the hypomyelination observed in PMLD patients.

Recently, complicated hereditary spastic paraplegia has been described as a new milder phenotype for C×47 mutation I33M.[8] The mutant formed homotypic gap junctional plaques in HeLa cells but formed altered heterotypic channels with C×43 in a cell model system. The authors predict that I33M causes loss of function mutation and disrupts GJIC via C×47/C×43 channels. If I33M has the same functional consequences as other mutations, another mechanism must account for the milder phenotype described.[8]

Finally, we could demonstrate a new alternative PMLD pathomechanism, namely a C×47 hemichannel dysfunction caused by a mutation localized in the C-terminus. Further studies on C-terminal mutations will contribute to a better understanding of pathomechanisms in PMLD.

CONFLICT OF INTEREST

The authors declare no conflict of interest.

ACKNOWLEDGEMENTS

We thank J Kaiser and I Markmann for technical assistance and H Werner and P De Monasterio for providing OLI-neu cells. This study was supported by the Deutsche Forschungsgemeinschaft grant number GA354/6-1 (to JG and MH).

1 Saugier-Veber P, Munnich A, Bonneau D *et al*: X-linked spastic paraplegia and Pelizaeus–Merzbacher disease are allelic disorders at the proteolipid protein locus. *Nat Genet* 1994; **6**: 257–262.

2 Schiffmann R, Boespflug-Tanguy O: An update on the leukodystrophies. *Curr Opin Neurol* 2001; **14**: 789–794.
3 Uhlenberg B, Schuelke M, Rüschendorf F *et al*: Mutations in the gene encoding gap junction protein alpha 12 (connexin 46.6) cause Pelizaeus–Merzbacher-like disease. *Am J Hum Genet* 2004; **75**: 251–260.
4 Bugiani M, Al Shahwan S, Lamantea E *et al*: GJA12 mutations in children with recessive hypomyelinating leukoencephalopathy. *Neurology* 2006; **67**: 273–279.
5 Salviati L, Trevisson E, Baldoin MC: A novel deletion in the *GJA12* gene causes Pelizaeus–Merzbacher-like disease. *Neurogenet* 2007; **8**: 57–60.
6 Wolf NI, Cundall M, Rutland P *et al*: Frameshift mutation in GJA12 leading to nystagmus, spastic ataxia and CNS dys-/demyelination. *Neurogenet* 2007; **8**: 39–44.
7 Henneke M, Combes P, Diekmann S *et al*: GJA12 mutations are a rare cause of Pelizaeus–Merzbacher-like disease. *Neurology* 2008; **70**: 748–754.
8 Orthmann-Murphy JL, Salsano E, Abrams CK *et al*: Hereditary spastic paraplegia is a novel phenotype for GJA12/GJC2 mutations. *Brain* 2009; **132**: 426–438.
9 Wang J, Wang H, Wang Y, Chen T, Wu X, Jiang Y: Two novel gap junction protein alpha 12 gene mutations in two Chinese patients with Pelizaeus–Merzbacher-like disease. *Brain Dev* 2009; **32**: 236–243.
10 Trosko JE, Ruch RJ: Cell–cell communication in carcinogenesis. *Front Biosci* 1998; **3**: D208–D236.
11 Kumar NM, Gilula NB: The gap junction communication channel. *Cell* 1996; **84**: 381–388.
12 Nagy JI, Dudek FE, Rash JE: Update on connexins and gap junctions in neurons and glia in the mammalian nervous system. *Brain Res Brain Res Rev* 2004; **47**: 191–215.
13 Rash JE, Yasumura T, Dudek FE, Nagy JI: Cell-specific expression of connexins and evidence of restricted gap junctional coupling between glial cells and between neurons. *J Neurosci* 2001; **21**: 1983–2000.
14 Massa PT, Mugnaini E: Cell junctions and intramembrane particles of astrocytes and oligodendrocytes: a freeze-fracture study. *Neuroscience* 1982; **7**: 523–538.
15 Nagy JI, Ochalski PAY, Li J, Hertzberg EL: Evidence for the colocalization of another connexin with connexin-43 at astrocytic gap junctionsin rat brain. *Neuroscience* 1997; **78**: 533–548.
16 Menichella DM, Goodenough DA, Sirkowski E, Scherer SS, Paul DL: Connexins are critical for normal myelination in the CNS. *J Neurosci* 2003; **23**: 5963–5973.
17 Odermatt B, Wellershaus K, Wallraff A *et al*: Connexin 47 (C×47)-deficient mice with enhanced green fluorescent protein reporter gene reveal predominant oligodendrocytic expression of cx47 and display vacuolized myelin in the cns. *J Neurosci* 2003; **23**: 4549–4559.
18 Giaume C, Fromaget C, El Aoumari A, Cordier J, Glowinski J, Gros D: Gap junctions in cultured astrocytes: single-channel currents and characterization of channel-forming protein. *Neuron* 1991; **6**: 133–143.
19 Nagy JI, Li X, Rempel J *et al*: Connexin26 in adult rodent central nervous system: demonstration at astrocytic gap junctions and colocalization with connexin30 and connexin43. *J Comp Neurol* 2001; **441**: 302–323.
20 Orthmann-Murphy JL, Freidin M, Fischer E, Scherer SS, Abrams CK: Two distinct heterotypic channels mediate gap junction coupling between astrocyte and oligodendrocyte connexins. *J Neurosci* 2007b; **27**: 13949–13957.
21 Orthmann-Murphy JL, Enriquez AD, Abrams CK, Scherer SS: Loss-of-function GJA12/Connexin47 mutations cause Pelizaeus-Merzbacher-like disease. *Mol Cell Neurosci* 2007a; **34**: 629–641.
22 Jung M, Krämer E, Grzenkowski M *et al*: Lines of murine oligodendroglial precursor cells immortalized by an activated neu tyrosine kinase show distinct degrees of interaction with axons *in vitro* and *in vivo*. *Eur J Neurosci* 1995; **7**: 1245–1265.
23 Barrio LC, Suchyna T, Bargiello T *et al*: Gap junctions formed by connexins 26 and 32 alone and in combination are differently affected by applied voltage. *Proc Natl Acad Sci USA* 1991; **88**: 8410–8414.
24 Barish ME: A transient calcium-dependent chloride current in the immature *Xenopus* oocyte. *J Physiol* 1983; **342**: 309–325.
25 Ebihara L: New roles for connexons. *News Physiol Sci* 2003; **18**: 100–103.
26 Kozak M: Interpreting cDNA sequences: some insights from studies. *Mamm Genome* 1996; **7**: 563–574.
27 Foote CI, Zhou L, Zhu X, Nicholson BJ: The pattern of disulfide linkages in the extracellular loop regions of connexin 32 suggests a model for the docking interface of gap junctions. *J Cell Biol* 1998; **140**: 1187–1197.
28 Dhaunchak AS, Nave KA: A common mechanism of PLP/DM20 misfolding causes cysteine-mediated endoplasmic reticulum retention in oligodendrocytes and Pelizaeus–Merzbacher disease. *Proc Natl Acad Sci USA* 2007; **104**: 17813–17818.
29 Olbina G, Eckhart W: Mutations in the second extracellular region of connexin43 prevent localization to the plasma membrane, but do not affect its ability to suppress cell growth. *Mol Cancer Res* 2003; **1**: 690–700.
30 Moreno AP, Lau AF: Gap junction channel gating modulated through protein phosphorylation. *Prog Biophys Mol Biol* 2007; **94**: 107–119.
31 Britz-Cunningham SH, Shah MM, Zuppan CW, Fletcher WH: Mutations of the connexin 43 gap-junction gene in patients with heart malformations and defects of laterality. *New Engl J Med* 1995; **332**: 1323–1329.
32 Omori Y, Mesnil M, Yamasaki H: Connexin 32 mutations from X-linked Charcot–Marie–Tooth disease patients: functional defects and dominant negative effects. *Mol Biol Cell* 1996; **7**: 907–916.
33 Castro C, Gómez-Hernandez JM, Silander K, Barrio LC: Altered formation of hemichannels and gap junction channels caused by C-terminal connexin32 mutations. *J Neurosci* 1999; **19**: 3752–3760.
34 Kondo RP, Wang SY, John SA, Weiss JN, Goldhaber JI: Metabolic inhibition activates a non-selective current through connexin hemichannels in isolated ventricular myocytes. *J Mol Cell Cardiol* 2000; **32**: 1859–1872.
35 Liang GS, de Miguel M, Gómez-Hernández JM *et al*: Severe neuropathy with leaky connexin32 hemichannels. *Ann Neurol* 2005; **57**: 749–754.
36 Deschênes SM, Walcott JL, Wexler TL, Scherer SS, Fischbeck KH: Altered trafficking of mutant connexin32. *J Neurosci* 1997; **17**: 9077–9084.
37 Orthmann-Murphy JL, Abrams CK, Scherer SS: Gap junctions couple astrocytes and oligodendrocytes. *J Mol Neurosci* 2008; **35**: 101–116.
38 Gow A, Lazzarini RA: A cellular mechanism governing the severity of Pelizaeus–Merzbacher disease. *Nat Genet* 1996; **13**: 422–428.
39 Gow A, Southwood CM, Lazzarini RA: Disrupted proteolipid protein trafficking results in oligodendrocyte apoptosis in an animal model of Pelizaeus–Merzbacher disease. *J Cell Biol* 1998; **140**: 925–934.
40 D'Urso D, Prior R, Greiner-Petter R, Gabreëls-Festen AA, Müller HW: Overloaded endoplasmic reticulum–Golgi compartments, a possible pathomechanism of peripheral neuropathies caused by mutations of the peripheral myelin protein PMP22. *J Neurosci* 1998; **18**: 731–740.
41 Aridor M, Balch WE: Integration of endoplasmic reticulum signaling in health and disease. *Nat Med* 1999; **5**: 745–751.
42 Gow A, Friedrich VL, Lazzarini RA: Many naturally occurring mutations of myelin proteolipid protein impair its intracellular transport. *J Neurosci Res* 1994; **37**: 574–583.

Supplementary Information accompanies the paper on European Journal of Human Genetics website (http://www.nature.com/ejhg)